

## Article

# In Vitro Biocompatibility Evaluation of a New Co-Cr-B Alloy with Potential Biomedical Application

María Cristina Garcia-Mendez <sup>1</sup>, Victor Hugo Urrutia-Baca <sup>2</sup>, Carlos A. Cuaó-Moreu <sup>3</sup> , Ernesto Lorenzo-Bonet <sup>3</sup> , Melvyn Alvarez-Vera <sup>3</sup>, David Mizael Ortiz-Martinez <sup>2</sup> and Myriam Angelica de la Garza-Ramos <sup>1,\*</sup> 

<sup>1</sup> Facultad de Odontología, Centro de Investigación y Desarrollo en Ciencias de la Salud/CIDICS, Universidad Autónoma de Nuevo León, San Nicolás de los Garza 64460, Mexico; cristina.garciamdz@uanl.edu.mx

<sup>2</sup> Facultad de Ciencias Biológicas, Universidad Autónoma de Nuevo León, San Nicolás de los Garza 66451, Mexico; victor.urrutiaba@uanl.edu.mx (V.H.U.-B.); dortizm@uanl.edu.mx (D.M.O.-M.)

<sup>3</sup> Facultad de Ingeniería Mecánica y Eléctrica, Universidad Autónoma de Nuevo León, San Nicolás de los Garza 66451, Mexico; carlos.cuaomr@uanl.edu.mx (C.A.C.-M.); ernesto.lorenzobnt@uanl.edu.mx (E.L.-B.); melvys1@yahoo.com.mx (M.A.-V.)

\* Correspondence: myriam.garzarm@uanl.edu.mx; Tel.: +52-818-329-4000 (ext. 1781)



**Citation:** Garcia-Mendez, M.C.; Urrutia-Baca, V.H.; Cuaó-Moreu, C.A.; Lorenzo-Bonet, E.; Alvarez-Vera, M.; Ortiz-Martinez, D.M.; de la Garza-Ramos, M.A. In Vitro Biocompatibility Evaluation of a New Co-Cr-B Alloy with Potential Biomedical Application. *Metals* **2021**, *11*, 1267. <https://doi.org/10.3390/met11081267>

Academic Editor: Changdong Gu

Received: 19 July 2021

Accepted: 6 August 2021

Published: 11 August 2021

**Publisher's Note:** MDPI stays neutral with regard to jurisdictional claims in published maps and institutional affiliations.



**Copyright:** © 2021 by the authors. Licensee MDPI, Basel, Switzerland. This article is an open access article distributed under the terms and conditions of the Creative Commons Attribution (CC BY) license (<https://creativecommons.org/licenses/by/4.0/>).

**Abstract:** Cobalt–chromium (Co-Cr) alloys have been used in a wide variety of biomedical applications, including dental, cardiovascular, and orthopedic devices. In vitro studies have shown that the mineralization of cells involved in osteogenesis is regulated by boron. The development of a new cobalt-chromium-boron (Co-Cr-B) alloy improves the mechanical properties of the metal, such as wear resistance, and meets biocompatibility requirements. Therefore, the objective of this study was to evaluate the osteogenic differentiation and biocompatibility in in vitro assays. Human dental pulp mesenchymal cells (hDPSCs) were isolated from volunteers and then co-cultured with the Co-Cr plus boron alloy from 0.3% to 1% for 15 days, while the formation of calcium deposits was quantified by Alizarin red staining and the expression of genes was related to osteodifferentiation by RT-qPCR. Simultaneously, the cytotoxicity of our alloy was evaluated by MTT assay and the change in the gene expression of cytokines commonly associated with inflammatory processes. The results showed low cytotoxicity when cells were treated with the Co-Cr-B alloy, and no change in the gene expression of IL-1 $\beta$ , TNF- $\alpha$ , IL-6, and IL-8 was observed compared to the untreated control ( $p > 0.05$ ). The osteoinduction results shown an increase in mineralization in hDPSCs treated with Co-Cr-B alloy with 1.0% B. In addition, a significant increase in mRNA levels for collagen type 1 in with 0.3% boron and alkaline phosphatase and Runx2 with 0.6% boron were observed. The addition of Boron to the ASTM F75 Co-Cr base alloy improves the biocompatible characteristics. No cytotoxicity and any change of the expression of the pro-inflammatory cytokines IL-1 $\beta$ , TNF- $\alpha$ , IL-6, and IL-8 in human peripheral blood mononuclear cells treated with the cobalt-chromium-boron alloy was observed in vitro assays. Furthermore, our alloy acts as an osteoinductive in osteogenic differentiation in vitro. Therefore, our results could set the standard for the development of in vivo trials and in the future, it could be considered as an alternative for regenerative therapy.

**Keywords:** boron; osteogenesis; implant; osteodifferentiation; alloy

## 1. Introduction

Stainless steel, titanium, and cobalt have been used as dental and medical prostheses in medicine and dentistry because they have fatigue resistance, are corrosion tolerant, and have good tissue compatibility [1–3]. They have been successfully used in hip and knee prostheses, bone plates, screws for fractures, and dental implants [4]. All of these have the purpose of improving the quality of life of patients who suffer lesions. However, infections, poor surgical procedures, biocompatibility, and material corrosion resulting from

colonization by microorganisms are still the subject of investigation. This research could help improve the biomechanical qualities and properties of the materials used today [5].

Regarding the colonization of microorganisms, it is known that dental biofilms can colonize dental implants that break the epithelial barrier. These implants are frequently reported as having a higher risk of dental infections (up to 90% of cases) [6]. It has been reported that endosteal implants have a success rate of 90 to 96% over ten years after being installed [7]. According to some scientific review studies, between 5 and 10% of cases of peri-implantitis have been reported worldwide [8].

On the other hand, the modifications to implants is an area of constant research in order to improve their properties. For example, the modification of endosteal implant surfaces has been shown to improve the integration of metal into bone tissue. Therefore, the development of dental implants and the search for biological principles that help understand and improve the dynamic process of the interface between bone tissue and the biomaterial are continuously evolving [9].

Among all metals, commonly, titanium (Ti) and its alloys are the material of choice for the manufacture of dental implants, but their cost is high. Likewise, since it is a material subjected to constant mechanical loads and chemical interactions in a dynamic environment such as the oral cavity, it is not exempt from failure.

Previous research aimed at exploring alternatives to titanium shows that the addition of boron leads to an increase in the wear resistance of cobalt-based alloys [10]. The increase in precipitates and the reduction in grain size produces a less severe abrasion wear mechanism. In addition, the interdendritic compounds that are formed exhibit resistance to defragmentation by retaining brittle fractures on the cobalt matrix. The effect decreases wear because these microstructures avoid carbide detachments, which is related to third-body abrasion and corrosion. Additionally, irritability tests in subcutaneous tissue of rats [11] revealed that Co-Cr alloys with added boron do not produce an inflammatory response of the tissues due to there not being evidence of macrophage cells.

It has been reported that cobalt is a metal that has been incorporated thanks to its antimicrobial properties. It has been combined with copper and tungsten (W), achieving a CoCrWCu alloy that is effective against bacteria such as *E. coli* [12]. In an in vitro model, a collagen scaffold with cobalt additions improved the angiogenic properties of cells and osteogenic differentiation [13].

Another metal is boron. A unique element essential for life, boron has physical and chemical properties that have encouraged its use as a key element for designing and developing new molecular technologies and therapeutic applications in medicine and biomaterial engineering [14]. Boron has been reported as a necessary trace element for optimal health as it plays vital roles in embryogenesis, osteogenesis, immune response, and psychomotor functions. New biomaterials, such as bioactive ceramics and glasses based on a borate or borosilicate composition, have been shown to induce bone formation [15]. Nielsen and Stoecker have confirmed that a dietary boron deficiency exhibits decreased bone volume compared to a diet rich in boron—3 mg/kg in rats. Boric acid has also been directly related to reducing periodontal inflammation and bone loss [16].

In dentistry, the mechanical properties of a chromium-cobalt alloy, including its hardness, resistance to tension, and corrosion resistance, determine its use as a metal of choice for dental implants [17]. The development of a new boron-added metal alloy at the School of Mechanical and Electrical Engineering of the Autonomous University of Nuevo Leon meets biocompatibility requirements and improves the mechanical properties of the metal, wear-resistance, and hardness [18,19].

The importance of this work lies in the in vitro evaluation of the behavior of this new Co-Cr-B alloy for the development of a dental implant that surpasses the characteristics of conventional implants through the possible osteogenic induction capacity conferred by the addition of boron. The hypothesis was that the addition of boron to our Co-Cr alloy would have biocompatibility and osteodifferentiation properties in an in vitro model.

## 2. Materials and Methods

### 2.1. Co-Cr-B Alloy Preparation

A cobalt-based alloy, ASTM F75, with 0.3%, 0.6%, and 1.0% boron was used. The alloy was machined into cylindrical pieces 9 mm in diameter by 4 mm in height. They were compared with Ti-6Al-4V cylinders of the same size. The Co-Cr-B cylinders were previously hot-mounted in Bakelite at 180 °C, 45 kN for 5 min. They were progressively polished with 320, 800, 1200, 2400, and 4000 sandpaper and finally with a cloth and alumina to obtain a mirror finish of the surfaces. They were cleaned with 75% alcohol and steam-sterilized at 15 pounds pressure for 20 min. The description of the employed samples is shown in Table 1.

**Table 1.** Description of the study samples.

Sample Name	Description
B0	ASTM F75 cobalt alloy without boron
B1	ASTM F75 cobalt alloy added with 0.3% boron
B2	ASTM F75 cobalt alloy added with 0.6% boron
B3	ASTM F75 cobalt alloy added with 1.0% boron
T0	Ti-6Al-4V alloy

### 2.2. Metallurgical and Microstructural Characterization

Scanning electron microscopy (SEM) observations of the samples were carried out in a JEOL JSM-6490LV (JEOL USA Inc., Peabody, MA, USA) apparatus operated in backscattering mode with energy-dispersive spectroscopy (EDS) to analyze the microstructure and chemical composition of the different phases of the alloys. Cobalt alloy samples were prepared by conventional metallography techniques and electrolytically etched with 90 mL HCl and 10 mL H<sub>2</sub>O for 5 s at 20 V [20].

#### 2.2.1. Chemical Characterization

X-ray diffraction patterns were obtained using a Panalytical Empyrean X-ray diffractometer (XRD, Malvern Panalytical, Malvern, Worcestershire, UK) with monochromatic Cu-K $\alpha$  radiation at  $\lambda = 1.54 \text{ \AA}$  by applying 45 kV and 40 mA over a range from 10° to 100°.

The elemental composition of the cobalt alloy with boron additions was determined by means of atomic emission spectroscopy.

#### 2.2.2. Hardness Test

The sample hardness was measured using the Vickers indentation test. An HMV-2 Shimadzu Microhardness Tester (Shimadzu Corporation, Nakagyo-ku, Kyoto, Japan) was used. Ten measurements were carried out per sample under an applied load of 1.961 N for 15 s following the ASTM E92 standard.

### 2.3. Extraction of Mesenchymal Stem Cells from Dental Pulp (hDPSCs)

Under sterile conditions, premolars were extracted from volunteer patients of the Orthodontic Postgraduate Program of the School of Dentistry of the Autonomous University of Nuevo Leon requiring premolar extractions due to orthodontic treatment. Atraumatic extractions were performed, meaning no gum flaps were raised during the extraction, and specialized extraction instruments known as periostomes were used so the socket and soft tissue were not harmed. The study was conducted in accordance with the Declaration of Helsinki, and the protocol was approved by the Ethics Committee of Universidad Autónoma de Nuevo León (SPSI-010613/00245). The sample was placed in a specific culture medium for transport. The isolation and characterization of human dental pulp mesenchymal cells (hDPSCs) continued.

The dental pulp was extracted by cutting the tooth at the level of the cemento-enamel junction with a low speed diamond burr and disk. Then, the pulp was detached from the pulp chamber and root canals with a probe. Once detached, the pulp was extracted with tweezers. Once the dental pulp was extracted, it was stored in sterile 15 mL tubes with Dulbecco's modified Eagle<sup>®</sup> culture medium (Thermo Fisher Scientific, Waltham, MA, USA) with low glucose supplementation (1 mg/mL) and antibiotics (100 U/mL penicillin, 100 µg/mL streptomycin, and 25 µg/mL amphotericin B). The pulp was transported at room temperature in a tube from the Periodontics Clinic to the Center for Research and Development in Health Sciences. Between pulp extraction and culture, there was a time range between one and twenty-four hours at 4 °C.

hDPSCs were isolated by enzymatic digestion (3 mg/mL collagenase type I and 4 mg/mL dispase) from human premolar teeth, isolated with CD271+, and cultured in DMEM supplemented with fetal bovine serum and antibiotics, as previously described by Del Angel-Moqueda et al. [21].

#### Cell Culture for Assays

Once the positive fraction of the hDPSCs was obtained, they were transferred to a 25 cm<sup>3</sup> T25 cell culture flask (Corning<sup>®</sup>, Corning, NY, USA); 5 mL of DMEM was added and incubated at a temperature of 37 °C in an atmosphere with 95% humidity and 5% CO<sub>2</sub>. From the suspension of DPSCs, cells were cultured in 24-well plates at a cell density of 20,000 cells/well and a final volume of 500 µL of Osteodiff<sup>®</sup> (Miltenyi Biotec, GmbH, Bergisch Gladbach, Germany). The following treatments were applied in duplicate for 15 days, monitoring and making changes in half every three days (Table 2).

**Table 2.** Treatments groups and description on hDPSCs.

Treatment Groups	Description
Positive control	Cells treated with Osteodiff <sup>®</sup>
Negative control	Cells treated with DMEM
Treatment 1	Titanium alloy
Treatment 2	(Co-Cr) alloy without boron
Treatment 3	(Co-Cr-B) with 0.3% of boron
Treatment 4	(Co-Cr-B) with 0.6% of boron
Treatment 5	(Co-Cr-B) with 1.0% of boron

Medium changes were made every 72 h until a cell confluence of 90% of the primary culture was obtained. The first passage was made to 2 flasks 25 cm<sup>3</sup>, and proliferation was monitored for 21 days until a confluence of 80% was obtained.

#### 2.4. Formation of Calcium Deposits by Alizarin Red Staining

After 15 days of osteogenic induction, the hDPSCs were washed with 1 mL of PBS; then, 1 mL of 10% formalin was added, and the cells were fixed for 1 h. The cells were rinsed with 1 mL of distilled water for 5 min, repeating this wash 2 times. The distilled water was decanted, and 500 µL of Alizarin red was added over 30 min. The staining was repeated and washed with 1 mL of distilled water for 3 min repeating the wash 3 times. The water was removed until the stained calcium deposits adhered to the bottom of the plate. The calcium deposits were measured at OD415 nm. The formation of calcium deposits in the treatments was compared with cells without treatment and treated with Osteodiff<sup>®</sup> as a negative and positive control of osteodifferentiation, respectively.

## 2.5. Assay of Gene Expression Related to Osteodifferentiation

### 2.5.1. RNA Extraction and cDNA Synthesis

The hDPSCs in suspension were separated by centrifugation at 1500 rpm for 10 min; then, it was washed with 1 mL of PBS and resuspended in 1 mL of Trizol (TRI Reagent<sup>®</sup>, Sigma-Aldrich, St. Louis, MI, USA) to ensure complete dissociation of the nucleoprotein complexes; these were incubated for 5 min at room temperature. Then, 0.2 mL of chloroform was added, mixed vigorously for 15 s, and incubated at room temperature for 15 min. The resulting mixture was centrifuged at 12,000 rpm for 15 min at 4 °C. Centrifugation separated the mixture into 3 phases: organic (proteins), interface (DNA), and aqueous superior (RNA).

The aqueous phase was transferred into a tube (Eppendorf, Hamburg, Germany) for RNA isolation, and 500 µL of 2-propanol was added for 10 min at room temperature. After incubation, the mixture was centrifuged at 12,000 rpm for 10 min at 4 °C. Subsequently, the supernatant was discarded, and the pellet was obtained, to which 1 mL of 75% ethanol was added; centrifugation was repeated to wash it. Finally, the ethanol contained in the sample was removed. The RNA was resuspended in nuclease-free water and stored at −80 °C until use. A total of 5 µL of RNA was diluted with 1 µL of 6× loading buffer. The mixture was loaded on 1% agarose gel in a 1× TBE buffer. The electrophoretic run was performed at 100 V for 45 min. It was stained in a solution of ethidium bromide (5 µg/mL). Finally, it was transferred to a Gel Doc<sup>™</sup> XR + Imager ultraviolet light transilluminator (Bio-Rad, Hercules, CA, USA). RNA, 1 µg, was used for cDNA synthesis using the M-MLV Reverse Transcriptase kit (Promega, Madison, WI, USA) following the manufacturer's recommendations.

### 2.5.2. Real-Time PCR

For the analysis of gene expression by real-time PCR, oligonucleotides targeting the alkaline phosphatase, Type 1 collagen, and Runx2 genes, and Beta Actin as a reference gene, were designed. The mRNA sequences were obtained from the GenBank database (NCBI). Runx2 Fwd: 5'-CTTCATTTGCACTGGGTCAC-3', Runx2 Rv: 5'-CTGCAAATCTCAGCCATGTT 3'; Type I collagen Fwd: 5'-ACCAACTGAACGTGACCAAAA-3', Type I collagen Rv: 5'-AGTGGGCAGAAAGGGACTTA-3'; osteocalcin Fwd: 5'-CTGCATCTGCTCTCTGAC-3', osteocalcin Rv: 5'-CCGGAGTCTATTACCACCT-3'; alkaline phosphatase Fwd: 5'-CGTCAATTAACGGCTGACAC-3', and alkaline phosphatase Rv: 5'-TCTGGCACAAATG AGTTGGT-3'.

The qPCR reactions were carried out in 96-well plates; 12.5 µL of Maxima Sybr Green/qPCR master mix 2× (Thermo-Scientific, Waltham, MA, USA), 3.32 µL of primer forward/reverse mix, 2 µL of cDNA, and 7.3 µL free water were used with nucleases at a final volume of 25 µL. The procedure was carried out in a LightCycler 480II thermal cycler (Roche, Basel, Switzerland), programmed with the Sybr Green I detection system in three stages; a pre-incubation cycle, 40 amplification cycles, a cycle for the melting curve, and a cooling cycle. The pre-incubation was at 95 °C for 10 min, and a decrease of 4 °C/s. Amplification was carried out with three temperatures: 95 °C for 10 s and a decrease of 4 °C/s, an alignment temperature as recommended by each pair of primers (52 °C) for 15 s and a decrease of 2 °C/s; finally at 72 °C for 10 s and a decrease of 4 °C/s in individual acquisition mode. The dissociation curve was at 95 °C for 5 s 4 °C/s, 65 °C for 1 min 2.2 °C/s, and finally, at 97 °C in continuous acquisition mode 5 °C. The cooling stage was 40 °C for 30 s and 1.5 °C/s for 2 s. Using relative expression analysis, the threshold cycle values (Cycle threshold Ct) and normalized radii were calculated by the  $\Delta\Delta C_t$  method using the LightCycler 480II (Roche, Basel, Switzerland), and Rest2009 software (v2.0.13, QIAGEN, Hilden, Germany); the relative expression is based on the expression ratio of a target gene versus a reference gene ( $\beta$ -actin). The gene expression values of treatments were compared with cells without treatment and treated with Osteodiff<sup>®</sup> (Miltenyi Biotec, GmbH, Bergisch Gladbach, Germany) as a negative and positive control of osteodifferentiation, respectively.

## 2.6. Isolation of Human Peripheral Blood Mononuclear Cells (hPBMCs)

hPBMCs have been widely used as an *in vitro* model to investigate biocompatibility and inflammation; thus, they were used in this work [22]. The hPBMCs were extracted using a density gradient [23]. Under sterile conditions, with a 10 mL serological pipet, 6 mL of whole blood was dispensed into a 15 mL conical bottom tube previously prepared with 6 mL of PBS, pH 7.4. The mixture of blood and PBS was homogenized by inversion; 9 mL of Ficoll-Hypaque™ PLUS® (GE Healthcare, Chicago, IL, USA) was dispensed into a 50 mL conical bottom tube. With a 1 mL pipet, 12 mL of the mixture of blood and PBS were slowly dispensed onto the wall of the tube without mixing with Ficoll so that two strata remained: the lower one with Ficoll-Hypaque™ PLUS® and the upper one with blood and PBS. It was centrifuged at 1400 rpm for 30 min at 20 °C without the handbrake. The conical bottom tube was removed from the centrifuge very carefully without disturbing the layers formed. With a 1 mL pipet, the layer corresponding to the MNCs was carefully aspirated and transferred to a 15 mL conical bottom tube. The tube was capped with the CMN at 10 mL with PBS, pH 7.4, and homogenized by inversion. It was centrifuged at 760 rpm for 15 min at 20 °C. The supernatant was discarded by decantation, and the cells were resuspended in 10 mL PBS, pH 7.4. It was centrifuged at 760 rpm for 15 min at 20 °C. Again, the supernatant was discarded by decantation, and the cells were resuspended in 10 mL PBS, pH 7.4. It was centrifuged at 760 rpm for 15 min at 20 °C. The supernatant was discarded by decantation, and 1 mL of supplemented RPMI culture medium (10% FBS, 100 U/mL penicillin, 100 µg/mL streptomycin, 1.25 µg/mL amphotericin, and 290 µg/mL glutamine) was added and the cells were resuspended with digital tapping.

## 2.7. Viability Assay on hPBMCs

The effect of the metal alloy Co-Cr-B on the viability in hPBMCs was evaluated by the LDH colorimetric method (LDH-Cytotoxicity Assay Kit II, Abcam, Cambridge, UK) in 96-well microplates, as previously reported by Szuhaneck et al. [24]. A cell suspension of isolated monocytes was cultured in 24-well microplates at a cell density of 710,000 cells/well and a final volume per well of 500 µL; the following treatments were applied in triplicate for 16 h, at 37 °C, 5% CO<sub>2</sub>. The treatments groups were as follows: Negative control: cells treated with DMEM; positive control 1: cells treated with 50 µL of lysis buffer for viability assay; positive control 2: cells treated with 100 ng/mL of LPS for inflammatory assay; treatment 5: Co-Cr-B alloy with 1% boron.

After 16 h, the cells were detached by pipetting, and the supernatant from each well was transferred to individual Eppendorf tubes and centrifuged at 1400 rpm for 10 min. An aliquot of 10 µL of the supernatant from each treatment was transferred to a 96-well microplate; 100 µL of WST Substrate Mix was mixed with 5 mL of LDH Assay Buffer; and 100 µL of this mixture was placed in each well. The plate was incubated for 30 min at room temperature. The microplate reading was performed at 450 nm on an iMark Microplate Reader Bio-Rad microplate reader (Bio-Rad, Hercules, CA, USA).

## 2.8. Inflammatory Response of PBMCs to Co-Cr-B Alloy Samples

The starting point was a 500,000 cell/mL suspension in 18 mL of supplemented RPMI. First,  $1 \times 10^6$  cell/mL were transferred for each treatment: Control-(untreated cells), Control + (100 ng/mL), and Treatment 5 (Co-Cr-B) in triplicate 6-well plates. These were incubated for 16 h, 37 °C, 5% CO<sub>2</sub>. The culture medium was removed, washed with PBS, trypsin was applied for 7 min, and the cells were transferred to a 1.5 mL conical bottom tube at 16 h post-treatment to proceed with the total RNA extraction.

The change of gene expression of interleukin 1 Beta (IL-1β), interleukin 6 (IL-6), interleukin 8 (IL-8), and tumor necrosis factor-alpha (TNF-α) in the PBMCs treated with (Co-Cr-B) alloy samples was evaluated; 100 ng/mL of LPS from *Escherichia coli* and RPMI were used as a positive control to induce an inflammatory response and negative control, respectively.

After 24 h of stimulation, total RNA from treated cells was extracted using Trizol (TRI Reagent; Sigma-Aldrich, St. Louis, MO, USA) according to the manufacturer's protocol. For the synthesis of complementary DNA, the M-MLV Reverse Transcriptase kit (Promega, Madison, WI, USA) was used following the instructions.

For quantitative PCR (qPCR), IL-1 $\beta$  fwd: 5'-CTCTCACCTCTCCTACTCACTT-3', IL-1 $\beta$  rv: 5'-TCAGAATGTGGGAGCGAATG-3'; IL-6 fwd: 5'-ACTCACCTCTTCAGAACGAATTG-3', IL-6 rv: 5'-CCATCTTTGGAAGGTTTCAGTTG-3'; Actin Beta fwd: 5'-GGCATCCTCACCCTGAAGTA-3' and Actin Beta rv: 5'-GGGGTGTGAAGGTCTCAA-3' primer sequences were used.

Each qPCR was prepared using 12.5  $\mu$ L of 2 $\times$  Maxima Sybr Green/qPCR master mix (Thermo-Scientific, Carlsbad, CA, USA), 0.5  $\mu$ M of forward/reverse primer mixture, 100 ng of cDNA, and nuclease-free water up to a final volume of 25  $\mu$ L were mixed in 96-well plates. The qPCR was run using a LightCycler 480II thermal cycler (Roche, Basel, Switzerland) with a four-step program: one cycle of pre-incubation, 50 cycles of amplification, one cycle for melting curve, and one cooling cycle. The pre-incubation was at 95  $^{\circ}$ C for 10 min and a ramp rate of 4  $^{\circ}$ C/s; each amplification cycle was carried out in three steps: the denaturing at 95  $^{\circ}$ C for 10 s and a ramp rate of 4  $^{\circ}$ C/s; the annealing temperature according to each primer pair for 15 s and a ramp rate of 2  $^{\circ}$ C/s, and the extension 72  $^{\circ}$ C for 10 s and a ramp rate of 4  $^{\circ}$ C/s in individual acquisition mode. The melting curve was at 95  $^{\circ}$ C for 5 s 4  $^{\circ}$ C/s, 65  $^{\circ}$ C for 1 min 2.2  $^{\circ}$ C/s, and 97  $^{\circ}$ C in continuous acquisition mode at 5  $^{\circ}$ C. The cooling was at 40  $^{\circ}$ C for 30 s with a ramp rate of 1.5  $^{\circ}$ C/s. For gene expression analysis, the cycle threshold (CT) values and the normalized relative expression ratio were calculated by the  $\Delta\Delta$ Ct method using LightCycler 480II software (v1.5, Roche, Basel, Switzerland) and Rest2009 (v2.0.13, QIAGEN, Hilden, Germany).

### 2.9. Statistical Analysis

The results were evaluated by an analysis of variance (ANOVA) to obtain the mean values and standard deviations. The differences between the control group and the treatments were compared using the Tukey test.

The medians and standard errors were calculated for gene expression analysis and plotted in a box-and-whisker plot. Differences were evaluated using the Mann-Whitney U test. A *p*-value < 0.05 was considered statistically significant in all treatments. The SPSS (v.22, IBM, North Castle, NY, USA) statistical package and Excel (2017, Microsoft, Redmond, WA, USA) were used.

## 3. Results

### 3.1. Metallurgical and Microstructural Characterization

SEM images from the B0, B1, B2, B3, and T0 samples are exhibited in Figure 1. Carbides inside the Co- $\alpha$  matrix, typical of the ASTM F-75 cobalt alloy microstructure, could be appreciated for the B0 (a) sample. The microstructural changes due to the boron addition could be observed for the B1 (b), B2 (c), and B3 (d) samples. The EDS analysis confirmed that the interdendritic network is rich in chromium and molybdenum. In the case of the T0 sample (e), the EDS showed the presence of Al and V in the Ti matrix.

### 3.2. Chemical Characterization

The patterns of the phases identified by XRD are shown in Figure 2. Characteristic peaks associated with the following phases were identified: (111) (200) face-centered cubic Co- $\alpha$ , (711) (Co-Cr-B)<sub>23</sub> C<sub>6</sub> carbides, and (411) (110) intermetallic  $\sigma$  compound (Co-Cr). In addition, the boron-containing patterns exhibited an orthorhombic Cr<sub>2</sub>B phase (131) and a cubic Co<sub>21</sub>Cr<sub>2</sub>B<sub>6</sub> phase (511). The elemental composition of each cobalt sample is exhibited in Table 3. The percentage of the boron content showed in Table 1 was confirmed.

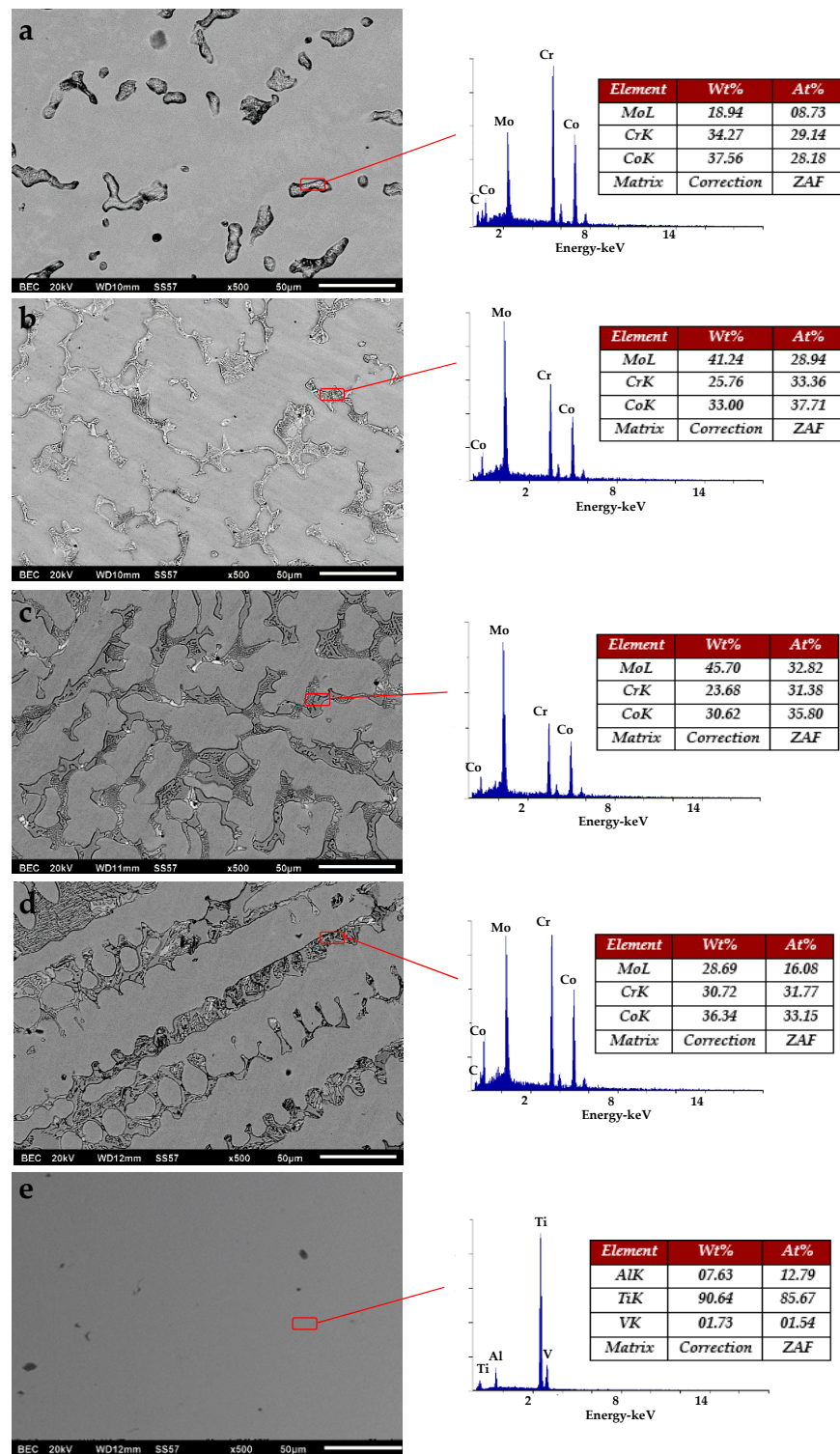
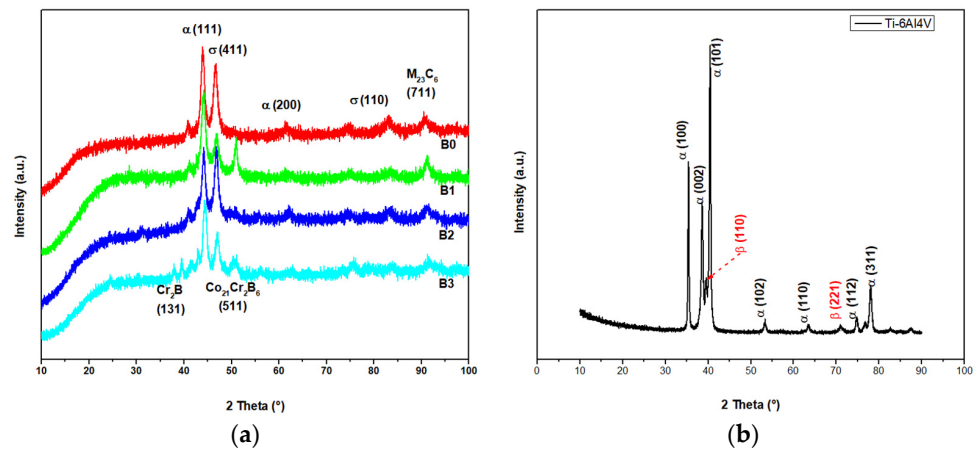


Figure 1. SEM images and EDS microanalysis of CoCr alloy with added boron: (a) sample B0, (b) sample B1, (c) sample B2, (d) sample B3, and (e) T0 sample.



**Figure 2.** X-ray diffraction patterns: (a) Co-Cr-B samples and (b) Ti-6Al-4V alloy.

**Table 3.** Chemical composition of cobalt samples in weight percentage (wt. %).

Element	B0	B1	B2	B3
Co	Bal.	Bal.	Bal.	Bal.
Cr	29.32	28.94	27.58	28.33
Mo	5.91	6.49	6.24	5.35
Ni	0.192	0.225	0.184	0.238
Fe	0.238	0.135	0.292	0.184
C	0.23	0.21	0.24	0.26
Si	0.28	0.58	0.43	0.63
Mn	0.43	0.14	0.23	0.46
W	0.15	0.09	0.11	0.13
N	0.09	0.12	0.18	0.16
Al	0.08	0.07	0.06	0.03
Ti	0.01	0.06	0.02	0.03
B	0.003	0.28	0.61	0.98

### 3.3. Hardness Test

The results of the hardness are shown in Figure 3. The B0 sample showed a hardness value around 35 HRC.

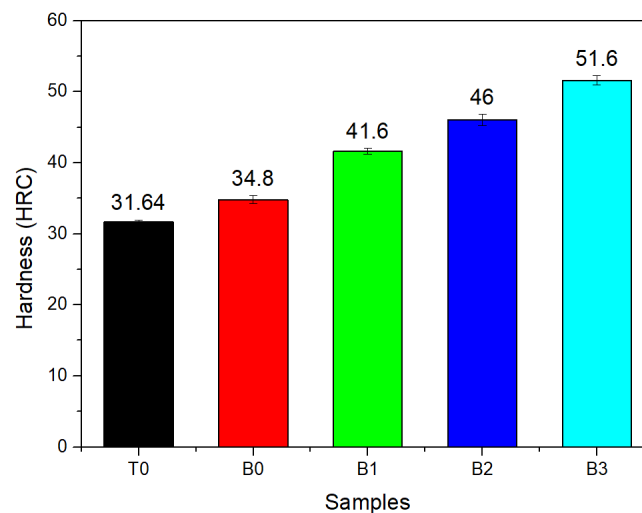


**Figure 3.** Microhardness of the Co-Cr samples with the variation of the percentage of boron and Ti-6Al-4V sample.

### 3.4. Cytotoxicity on hPBMCs

The cytotoxicity of the Co-Cr-B alloy and 100 ng/mL LPS on hPBMCs was evaluated by lactate dehydrogenase assay with regard to the internal positive control (lysis buffer; 1% triton x-100) and negative control (untreated cells). The results showed low cytotoxicity with  $2.83 \pm 4.6\%$  when treated with the Co-Cr-B alloy and  $2.50 \pm 4.7\%$  when was treated with LPS; no statistical differences were observed in these treatments compared to the negative control ( $p > 0.05$ ). All cytotoxicity results are shown in Figure 4.

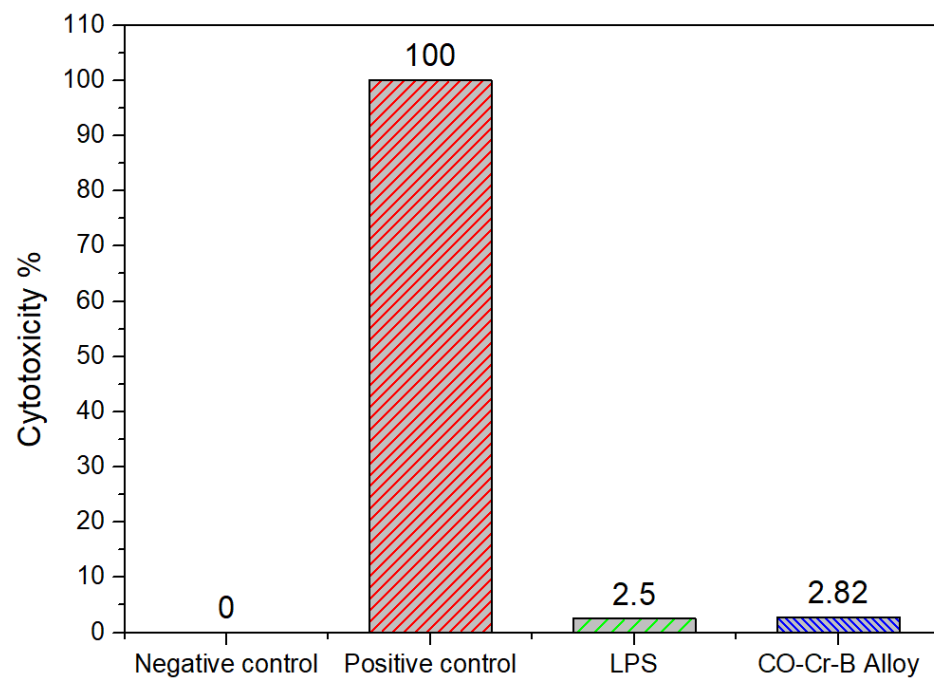


**Figure 4.** Percentage of cytotoxicity of chromium-cobalt-boron alloy on human peripheral blood mononuclear cells (hPBMCs). Data are shown as the mean  $\pm$  standard deviation of the percentage of cytotoxicity by LDH assay. Positive control—1% Triton x-100; Negative control—untreated cells; LPS—lipopolysaccharide from *E. coli*; Co-Cr-B alloy—chromium-cobalt-boron alloy.

### 3.5. Inflammatory Response of hPBMCs to Cr-Co-B Alloy

The relative quantification of mRNA for the pro-inflammatory cytokines IL-1 $\beta$ , TNF- $\alpha$ , IL-6, and IL-8 was carried out in human peripheral blood mononuclear cells stimulated with LPS and the Co-Cr-B alloy by RT-qPCR. Furthermore, the Ct (Cycle threshold) and normalized R<sub>adj</sub> values were obtained by the  $\Delta\Delta$ Ct method.

A significant increase in mRNA levels for IL-1 $\beta$ , TNF- $\alpha$ , IL-6, and IL-8 was observed on hPBMCs treated with LPS compared to the control of untreated cells ( $p < 0.05$ ). On the other hand, no significant difference was observed in IL-1 $\beta$ , TNF- $\alpha$ , IL-6, and IL-8 expression when cells were treated with the Co-Cr-B alloy with regard to the untreated control ( $p > 0.05$ ); the data are shown in Table 4.

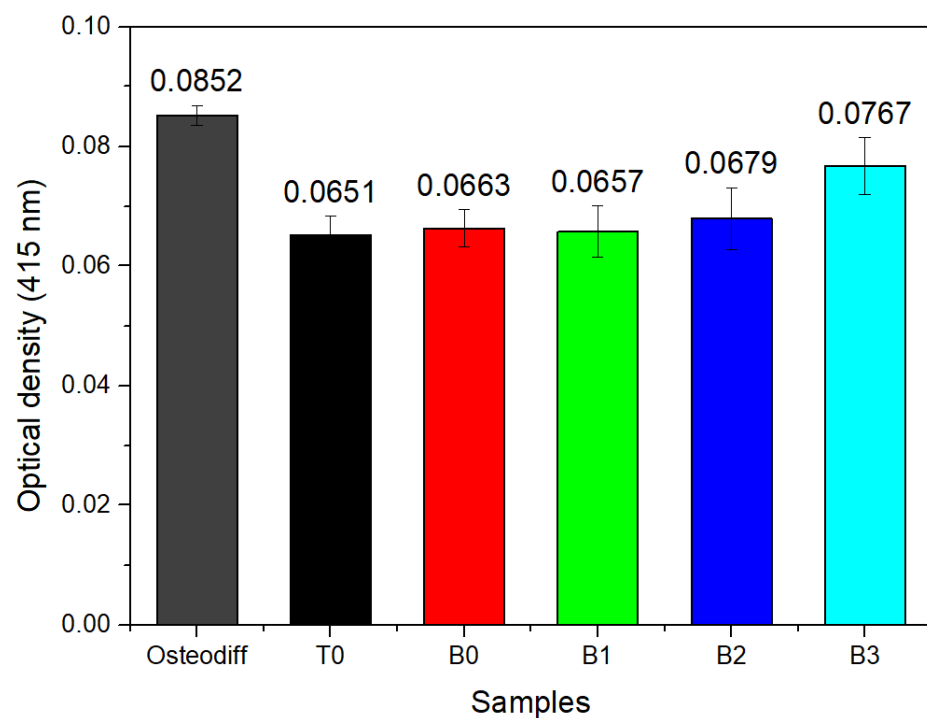
### 3.6. Formation of Extracellular Calcium Deposits in MSC Stimulated with the Co-Cr-B Alloy

The cell differentiation capacity of the DPSC lineage was evaluated in the presence of the Co-Cr alloy with different concentrations of B, 0.3%, 0.6%, and 1.0%. The dissolution of extracellular calcium deposits stained with Alizarin red was quantified by optical density (OD) at 415 nm in an Imark microplate reader (Bio-Rad, Hercules, CA, USA).

The analysis showed the following results: in the Osteodiff treatment (positive control), the OD average was  $0.0852 \pm 0.0017$ ; T0:  $0.0651 \pm 0.0033$ ; B0:  $0.0663 \pm 0.0033$ ; B1:  $0.0657 \pm 0.0045$ ; B2:  $0.0679 \pm 0.0055$  and B3:  $0.0767 \pm 0.005$  (Figure 5).

**Table 4.** Relative expression of IL-1 $\beta$ , TNF- $\alpha$ , IL-6, and IL-8 genes of hPBMCs treated with Cr-Co-B alloy.

Treatment	Relative Expression	Standard Error	95% C.I.	<i>p</i> Value	Result
IL-1 $\beta$					
Calibrator normalized	1.0	-	-	-	-
LPS	3.706	2.342–5.799	1.965–7.134	0.004	UP
Co-Cr-B alloy	0.58	0.359–0.882	0.309–1.132	0.15	No change
TNF- $\alpha$					
Calibrator normalized	1.0	-	-	-	-
LPS	2.255	1.451–3.366	1.265–4.983	0.003	UP
Co-Cr-B alloy	0.822	0.586–1.357	0.518–1.536	0.473	No change
IL-6					
Calibrator normalized	1.0	-	-	-	-
LPS	74.543	60.055–105.514	57.452–112.396	0.001	UP
Co-Cr-B alloy	2	1.587–2.845	1.485–3.079	0.065	No change
IL-8					
Calibrator normalized	1.0	-	-	-	-
LPS	4.297	2.688–9.130	2.312–10.388	0.001	UP
Co-Cr-B alloy	1.526	0.966–3.134	0.873–3.631	0.332	No change

**Figure 5.** Quantification of extracellular calcium deposits in MSC stimulated with the Cr-Co-B alloy by Alizarin red staining. The data shown as mean  $\pm$  standard deviation of optical density values at 415 nm. The OD<sub>415 nm</sub> are directly proportional to the formation of calcium deposits because they were solubilized and measured by spectrophotometry.

The highest amount of calcium deposits compared to all treatments were found in the control group, as expected. Among the experimental groups, no statistically difference was observed between Co-Cr-B with 1.0% B group (B3) and the positive control with a  $p = 0.44$ . In addition, a significant difference was also demonstrated for the B3 group, compared to the T0, B0, B1, and B2 groups ( $p \leq 0.0001$ ).

### 3.7. The mRNA Expression of Mineralization-Related Genes on MSCs

Relative quantification of mRNA was performed for the Runx2, alkaline phosphatase, and type I collagen genes in DPSCs stimulated with the Co-Cr-B alloy by RT-qPCR. Data are shown as the median of the normalized ratio  $\pm$  standard error. A significant increase in mRNA levels for COL I was observed in B1-treated cells relative to untreated control cells. A significant increase in the mRNA levels for AF and Runx2 was observed in cells treated with B2 compared to the control of untreated. A significant increase in the mRNA levels for AF, COL I, and Runx2 was observed in cells treated with osteodiff, as expected (Table 5). The effect of boron on gene expression was not dose dependent.

**Table 5.** Relative expression of collagenase, alkaline phosphatase, and Runx2 genes on human mesenchymal stem cells from dental pulp (hDPSCs) treated with Cr-Co-B alloy.

Treatment	Relative Expression	Standard Error	p-Value	Result
Type 1 collagen				
Calibrator normalized	1.0	-	-	-
Osteodiff	26.4	24.613–27.331	0.001	UP
T0	2.1	1.980–2.341	0.330	No regulation
B0	0.842	0.745–0.941	0.064	No regulation
B1	232.862	120.53–245.170	0.026	UP
B2	0.956	0.032–0.054	0.945	No regulation
B3	0.875	0.454–0.966	0.854	No regulation
Alkaline phosphatase				
Calibrator normalized	1.0	-	-	-
Osteodiff	28.4	27.820–30.493	0.001	UP
T0	0.0001	0.000–0.000	0.018	Down
B0	0.0001	0.000–0.000	0.000	Down
B1	1.101	0.0452–1.241	0.529	No regulation
B2	17.877	11.570–34.224	0.009	UP
B3	0.057	0.038–0.107	0.000	Down
Runx2				
Calibrator normalized	1.0	-	-	-
Osteodiff	34.3	29.430–35.534	0.001	UP
T0	1.02	0.976–1.120	0.081	No regulation
B0	0.003	0.001–0.010	0.032	Down
B1	0.802	0.032–1.101	0.344	No regulation
B2	9.624	3.383–33.344	0.000	UP
B3	0.943	0.701–1.196	0.732	No regulation

#### 4. Discussion

A possible boron-carbon network of  $\text{Co}_x\text{-B}_x$ ,  $\text{Cr}_x\text{-B}_x$ ,  $\text{Mo}_x\text{-B}_x$ , and  $\text{B}_x\text{C}_x$  could be identified for the B2 and B3 samples. According to previous authors [19,25–27], carbon could be partially substituted by boron, resulting in the formation of different compounds. In addition, this network exhibited a preferential alienation into interdendritic and grain boundaries (B3 sample). In addition, microporosity due to the casting process at high temperatures could be appreciated. The formation of boron carbides was confirmed by XRD [19]. In addition, the increment of the percentage of boron led to a displacement of the diffraction peaks to the right due to a distortion of the crystalline structure of the alloy. Additionally, characteristic peaks can be observed at angles  $2\theta$  of  $35.30^\circ$ ,  $38.43^\circ$ ,  $40.41^\circ$ ,  $53.21^\circ$ ,  $63.20^\circ$ ,  $76.08^\circ$ , and  $77.54^\circ$  associated with planes (100), (002), (101), (102), (110), (112), and (311) corresponding to a hexagonal Ti- $\alpha$  phase. In addition, a Ti- $\beta$  phase was identified at the planes (110) and (221) [28]. Hardness was increased by increasing the boron content in the cobalt alloy. The formation of boron carbides enhanced the interdendritic network of the alloy, which caused a reduction in grain size (Figure 1) and an increase in hardness. On the other hand, the T0 sample showed a hardness value of 31.64 HRC, which is lower than that of the Co-Cr samples.

It has been shown that the mineralization of cells involved in osteogenesis is affected by the presence or absence of boron. In an *in vitro* study by Taşlı et al., the odontogenic and osteogenic differentiation capacity of mesenchymal cells isolated from dental germ stem cells (hTGSCs) cultured with different concentrations of sodium pentaborate pentahydrate (borax) was evaluated. The results obtained showed that the cells treated with B showed an increase in alkaline phosphatase activity and the expression of genes related to odontogenesis and osteogenesis compared to the control group without treatment [16].

Hakki et al. investigated the effects of B on the cell survival, proliferation, mineralization, and mRNA expression of mineralized tissue-associated proteins and the effects of B on the BMP-4, -6 and -7 protein levels of pre-osteoblastic cells (MC3T3-E1). In the short term, a decreased cell survival rate was observed at 1000 ng/mL B and above. On the other hand, the results showed that 1 and 10 ng/mL of BA increased the mineralization of nodules, and the mRNA overexpression of type I collagen, osteopontin, bone sialoprotein, osteocalcin, and RunX was observed in all B treatment groups in comparison with untreated control. They also found that BA supplementation increased the bone morphogenetic proteins 4, 6, and 7 [29]. In our study, we found that the Co-Cr alloy with 1% boron did not significantly affect cell viability.

Ying et al. demonstrated that the proliferation of human bone marrow mesenchymal cells (BMSCs) was not affected by the treatment of 10 and 100 ng/mL of BA. In contrast, these concentrations caused an elevation in alkaline phosphatase (ALP) activity and increased mRNA expression levels of ALP, osteocalcin, type I collagen, and bone morphogenetic protein 7 (BMP-7) [30]. They observed a significant overexpression of these genes from the fourth day when the cells were treated with 10 ng/mL and 100 ng/mL of boron. In our study, we observed an overexpression of COL I gene when our alloy with 0.3% boron and the Runx2 and ALP genes with 0.6% boron were evaluated.

Najafabadi et al. demonstrated that the mineralization of rat bone marrow mesenchymal cells cultured with different concentrations of boric acid begins on the fifth day and increases significantly until the 21st day. Compared to the control group, in the absence of boric acid, mineralization begins on day 10 and continues until 15 or 21 days. These results suggest that boron may be a factor involved in the more accelerated response of osteogenic differentiation expression [31]. The gene expression and mineralization analysis of our study was determined at 15 days.

Another fact that relates boron to mineral metabolism is that after a period of deficit in the dietary intake of boron, the urinary excretion of hydroxyproline increases during the period of boron shortage. This finding suggests that boron increases collagen turnover since, usually, increased hydroxyprolinuria has been related to collagen degradation and loss of bone mass, which is consistent with the idea that boron has a positive effect on

bone metabolism. However, urinary hydroxyproline comes not only from the destruction of collagen but also from collagen synthesis during the breaking down of the N-terminal peptides of pre-collagen. Therefore, it may be possible that boron increases bone formation, causing a greater need for collagen and a greater synthesis, and as a result, an increase in hydroxyprolinuria occurs.

Regarding cell viability, rat bone marrow mesenchymal cells were exposed for 12 h to a low dose of 6 ng/mL of BA. Their viability was not affected; however, with higher exposure for 24 and 36 h, there was a decrease in metabolic activity and viability. Additionally, it was shown that cells in culture with a dose of 6 ng/mL of boron increased alkaline phosphatase activity levels and total calcium concentration [31].

Witek et al. evaluated the *in vitro* osseointegration of endosseous titatin type II implants by boronizing their surface using acid etching and machining until achieving a layer of 10–15  $\mu\text{m}$  boron particles. In their results, the fraction of area occupied by bone was not statistically significant compared to the control group at 3 weeks. These results are not consistent with the *in vitro* results that describe the regenerative properties of boron, so it is suggested to continue investigating [32].

The addition of boron to a nanogel scaffold improved the mechanical properties compared to the nanogel without boron. These scaffolds were implanted in bone defects in the femur of rats, and hematoxylin and eosin stains were performed to evaluate new bone formation. Histological analysis demonstrated trabecular bone formation and increased bone density at 4 weeks and the formation of new disorganized blood vessels in the area of the defect. They also demonstrated that osteoblasts grown in the presence of boron demonstrated a higher proliferation rate and increased expression levels of collagen type I and Runx-2 genes [33].

In this study, the effects of boron-added ASTM F75 cobalt-base alloy on the gene expression of IL-1 $\beta$ , IL-6, IL-8, TNF- $\alpha$  in mononuclear cells isolated from peripheral blood were evaluated. The results obtained show that there is no significant effect on the expression of the mentioned genes.

In contrast to a study suggesting that boron induces lymphocyte proliferation in the inflammatory process, our study evaluated the toxic effects of boron-added ASTM F75 cobalt-base alloy on mononuclear cells isolated from human peripheral blood by quantification of lactate dehydrogenase (LDH) and pro-inflammatory cytokine gene expression: IL-1 $\beta$ , IL-6, IL-8, TNF- $\alpha$  by real-time PCR. The results obtained showed low cytotoxicity on CMN with a mean value of 2.83% when treated with the chromium-cobalt-boron alloy for 16 h. Gene expression analysis revealed no significant overexpression of genes encoding IL-1 $\beta$ , IL-6, IL-8, and TNF- $\alpha$  in cells treated with the alloy compared to untreated cells. Therefore, the addition of boron to the base alloy cobalt-chromium ASTM F75 did not show cytotoxicity in PBMCs nor did it modify the expression of pro-inflammatory cytokines; therefore, it can be considered a biocompatible alloy of choice for the manufacture of biomedical devices in the area of implantology [34].

There are reports where the cytotoxicity of the Co-Cr-Mo alloy has been evaluated. The researchers observed notable cytotoxicity with the MTT assay of the Co-Cr-Mo alloy on primary culture of human fibroblasts from a gingival tissue biopsy [35].

Our results agree with a study carried out at the University of Alabama, Birmingham, where no changes were observed in the morphology and viability of gingival fibroblasts exposed to the base nickel and chromium alloy [36].

In an *in vitro* study in 1996, none of the metal ions (Au, Ag, Cu, Hg, Ni) to which monocytes were exposed for 24 h caused changes in the levels of IL-1B and TNF-alpha in the absence of LPS and the cells treated with LPS; the increase was as expected, but the release was greater in IL-1B [37].

Among the main alloys used for the manufacture of prostheses, there is stainless steel type AISI 316L. In an *in vitro* study, the levels of TNF- $\alpha$  and IL-1B always increased when peripheral blood monocytes were cultured in the presence of the AISI 316L alloy samples (stainless steel) compared to the control. In addition, a significant increase in the release

of LDH was observed in the same cell culture in the presence of samples treated with a collagen coating compared to the control, unlike the samples without coating in which there was no significant difference in LDH release. They also reported that the proliferation and release of LDH from human mononuclear cells isolated from peripheral blood is not affected by incubation with metallic samples compared to the control, so it is suggested that there is good cell viability [38].

In contrast, the cytokines analyzed in this work showed a different behavior from the results obtained in an in vitro study where researchers demonstrated that the Co-Cr alloy releases metal ions that sensitize Th1 lymphocytes, increasing the production of cytokines mediating bone resorption, and as a consequence, causing the rejection of the prosthesis [36].

It is desirable to explore whether our findings are replicable in other cell lines such as human osteoblasts. Furthermore, results derived from in vitro tests can be a good predictor of events that may occur in in vivo animal models; however, this approach needs to be explored.

## 5. Conclusions

The addition of boron to the ASTM F75 cobalt-chromium base alloy improves biocompatible characteristics. No cytotoxicity and any change of the expression of the pro-inflammatory cytokines IL-1 $\beta$ , TNF- $\alpha$ , IL-6, and IL-8 in human peripheral blood mononuclear cells treated with the cobalt-chromium-boron alloy was observed in in vitro assays. Furthermore, our alloy acts as an osteoinductive in osteogenic differentiation in vitro, since it showed an increase in the mineralization of extracellular calcium deposits and induction of the expression of genes related to osteogenic differentiation. Therefore, our results could set the standard for the development of in vivo trials, and in the future, it could be considered as an alternative for regenerative therapy.

**Author Contributions:** Conceptualization, M.C.G.-M., C.A.C.-M. and E.L.-B.; methodology, V.H.U.-B. and D.M.O.-M.; validation, M.A.d.I.G.-R. and M.A.-V.; formal analysis, M.C.G.-M., C.A.C.-M., E.L.-B., V.H.U.-B., D.M.O.-M. and M.A.d.I.G.-R.; investigation, M.C.G.-M., M.A.-V. and M.A.d.I.G.-R.; resources, M.A.d.I.G.-R., C.A.C.-M. and E.L.-B.; data curation, C.A.C.-M. and E.L.-B.; writing—original draft preparation, review and editing, M.C.G.-M., M.A.-V. and V.H.U.-B.; supervision and project administration, M.A.d.I.G.-R., C.A.C.-M. and E.L.-B. All authors have read and agreed to the published version of the manuscript.

**Funding:** This research received no external funding.

**Institutional Review Board Statement:** The study was conducted according to the guidelines of the Declaration of Helsinki, and approved by the Ethics Committee of Universidad Autónoma de Nuevo León (protocol code SPSI-010613/00245; 02/05/2018).

**Data Availability Statement:** Data presented in this article are available at request from the corresponding author.

**Acknowledgments:** We thank Sergio Lozano-Rodriguez for his help in reviewing and editing the manuscript.

**Conflicts of Interest:** The authors declare no conflict of interest.

## References

1. Saini, M. Implant biomaterials: A comprehensive review. *World J. Clin. Cases* **2015**, *3*, 52–57. [[CrossRef](#)] [[PubMed](#)]
2. Eliaz, N. Corrosion of Metallic Biomaterials: A Review. *Materials* **2019**, *12*, 407. [[CrossRef](#)]
3. Tribst, J.P.M.; de Oliveira Dal Piva, A.M.; Lo Giudice, R.; Borges, A.L.S.; Bottino, M.A.; Epifania, E.; Ausiello, P. The Influence of Custom-Milled Framework Design for an Implant-Supported Full-Arch Fixed Dental Prosthesis: 3D-FEA Study. *Int. J. Environ. Res. Public Health* **2020**, *17*, 4040. [[CrossRef](#)] [[PubMed](#)]
4. Pacifici, L. Metals Used in Maxillofacial Surgery. *Oral Implant.* **2016**, *9*, 107–111. [[CrossRef](#)]
5. Zhang, E.; Zhao, X.; Hu, J.; Wang, R.; Fu, S.; Qin, G. Antibacterial metals and alloys for potential biomedical implants. *Bioact. Mater.* **2021**, *6*, 2569–2612. [[CrossRef](#)] [[PubMed](#)]

6. Grischke, J.; Eberhard, J.; Stiesch, M. Antimicrobial dental implant functionalization strategies—A systematic review. *Dent. Mater. J.* **2016**, *35*, 545–558. [[CrossRef](#)]
7. Raikar, S.; Talukdar, P.; Kumari, S.; Panda, S.K.; Oommen, V.M.; Prasad, A. Factors affecting the survival rate of dental implants: A retrospective study. *J. Int. Soc. Prev. Community Dent.* **2017**, *7*, 351–355. [[CrossRef](#)]
8. Norowski, P.A.; Bumgardner, J.D. Biomaterial and antibiotic strategies for peri-implantitis: A review. *J. Biomed. Mater. Res. Part B Appl. Biomater.* **2009**, *88*, 530–543. [[CrossRef](#)]
9. Przekora, A. Current Trends in Fabrication of Biomaterials for Bone and Cartilage Regeneration: Materials Modifications and Biophysical Stimulations. *Int. J. Mol. Sci.* **2019**, *20*, 435. [[CrossRef](#)] [[PubMed](#)]
10. Alvarez-Vera, M.; Ortega, J.; Hernandez-Rodriguez, M.A.L. A study of the wear performance in a hip simulator of a metal–metal Co–Cr alloy with different boron additions. *Wear* **2013**, *301*, 175–181. [[CrossRef](#)]
11. Alvarez-Vera, M.; Juarez-Hernandez, A.; Gonzalez-Rivera, C.; Mercado-Solis, R.D.; Hernandez-Rodriguez, M. Biotribological response of Co Cr alloy with added boron under ball-on-disc tests. *Wear* **2013**, *301*, 243–249. [[CrossRef](#)]
12. Lu, Y.; Ren, L.; Wu, S.; Yang, C.; Lin, W.; Xiao, S.; Yang, Y.; Yang, K.; Lin, J. CoCrWCu alloy with antibacterial activity fabricated by selective laser melting: Densification, mechanical properties and microstructural analysis. *Powder Technol.* **2018**, *325*, 289–300. [[CrossRef](#)]
13. Perez, R.; Kim, J.-H.; Buitrago, J.O.; Wall, I.B.; Kim, H.-W. Novel therapeutic core–shell hydrogel scaffolds with sequential delivery of cobalt and bone morphogenetic protein-2 for synergistic bone regeneration. *Acta Biomater.* **2015**, *23*, 295–308. [[CrossRef](#)]
14. Icten, O.; Hosmane, N.S.; Kose, D.A.; Zumreoglu-Karan, B. Production of Magnetic Nano-bioconjugates via Ball Milling of Commercial Boron Powder with Biomolecules. *Z. Anorg. Allg. Chem.* **2016**, *642*, 828–832. [[CrossRef](#)]
15. Rahaman, M.N.; Day, D.E.; Bal, B.S.; Fu, Q.; Jung, S.B.; Bonewald, L.F.; Tomsia, A.P. Bioactive glass in tissue engineering. *Acta Biomater.* **2011**, *7*, 2355–2373. [[CrossRef](#)]
16. Taşlı, P.N.; Doğan, A.; Demirci, S.; Şahin, F. Boron Enhances Odontogenic and Osteogenic Differentiation of Human Tooth Germ Stem Cells (hTGSCs) In Vitro. *Biol. Trace Element Res.* **2013**, *153*, 419–427. [[CrossRef](#)] [[PubMed](#)]
17. Mavrogenis, A.F.; Papagelopoulos, P.J.; Babis, G.C. Osseointegration of Cobalt–Chrome Alloy Implants. *J. Autom. Inf. Sci.* **2011**, *21*, 349–358. [[CrossRef](#)] [[PubMed](#)]
18. Hakki, S.S.; Dundar, N.; Kayis, S.A.; Hakki, E.E.; Hamurcu, M.; Kerimoglu, U.; Baspinar, N.; Basoglu, A.; Nielsen, F.H. Boron enhances strength and alters mineral composition of bone in rabbits fed a high energy diet. *J. Trace Elem. Med. Biol.* **2013**, *27*, 148–153. [[CrossRef](#)]
19. Hernandez-Rodriguez, M.A.; Laverde-Cataño, D.A.; Lozano, D.; Martinez-Cazares, G.; Bedolla-Gil, Y. Influence of Boron Addition on the Microstructure and the Corrosion Resistance of CoCrMo Alloy. *Materials* **2019**, *9*, 307. [[CrossRef](#)]
20. Vander Voort, G.F. *Metallography, Principles and Practice*; ASM International: Materials Park, OH, USA, 1999; p. 1821.
21. Del Angel-Mosqueda, C.; Gutierrez-Puente, Y.; López-Lozano, A.P.; Romero-Zavaleta, R.E.; Mendiola-Jiménez, A.; La Garza, C.E.M.-D.; Marquez-M, M.; De La Garza-Ramos, M.A. Epidermal growth factor enhances osteogenic differentiation of dental pulp stem cells in vitro. *Head Face Med.* **2015**, *11*, 29. [[CrossRef](#)] [[PubMed](#)]
22. Chen, R.; Curran, J.; Pu, F.; Zhuola, Z.; Bayon, Y.; Hunt, J.A. In Vitro Response of Human Peripheral Blood Mononuclear Cells (PBMC) to Collagen Films Treated with Cold Plasma. *Polymers* **2017**, *9*, 254. [[CrossRef](#)]
23. Fuss, I.J.; Kanof, M.E.; Smith, P.D.; Zola, H. Isolation of Whole Mononuclear Cells from Peripheral Blood and Cord Blood. *Curr. Protoc. Immunol.* **2009**, *85*, 7.1.1–7.1.8. [[CrossRef](#)]
24. Szuhanek, C.A.; Watz, C.G.; Avram, Ş.; Moacă, E.-A.; Mihali, C.V.; Popa, A.; Campan, A.A.; Nicolov, M.; Dehelean, C.A. Comparative Toxicological In Vitro and In Ovo Screening of Different Orthodontic Implants Currently Used in Dentistry. *Materials* **2020**, *13*, 5690. [[CrossRef](#)] [[PubMed](#)]
25. Ferrari, V.; Wolf, W.; Zepon, G.; Coury, F.; Kaufman, M.; Bolfarini, C.; Kiminami, C.; Botta, W. Effect of boron addition on the solidification sequence and microstructure of AlCoCrFeNi alloys. *J. Alloys Compd.* **2019**, *775*, 1235–1243. [[CrossRef](#)]
26. Birmingham, M.J.; McDonald, S.; StJohn, D.; Dargusch, M. The effect of boron on the refinement of microstructure in cast cobalt alloys. *J. Mater. Res.* **2011**, *26*, 951–956. [[CrossRef](#)]
27. Rogl, P.; Korniyenko, K.; Velikanova, T. Boron–Carbon–Molybdenum. *Landolt Börnstein* **2009**, *11*, 422.
28. Deng, G.; Zhao, X.; Su, L.; Wei, P.; Zhang, L.; Zhan, L.; Chong, Y.; Zhu, H.; Tsuji, N. Effect of high pressure torsion process on the microhardness, microstructure and tribological property of Ti6Al4V alloy. *J. Mater. Sci. Technol.* **2021**, *94*, 183–195. [[CrossRef](#)]
29. Hakki, S.S.; Bozkurt, B.S.; Hakki, E.E. Boron regulates mineralized tissue-associated proteins in osteoblasts (MC3T3-E1). *J. Trace Elem. Med. Biol.* **2010**, *24*, 243–250. [[CrossRef](#)] [[PubMed](#)]
30. Ying, X.; Cheng, S.; Wang, W.; Lin, Z.; Chen, Q.; Zhang, W.; Kou, D.; Shen, Y.; Cheng, X.; Rompis, F.A.; et al. Effect of Boron on Osteogenic Differentiation of Human Bone Marrow Stromal Cells. *Biol. Trace Elem. Res.* **2011**, *144*, 306–315. [[CrossRef](#)]
31. Najafabadi, B.-A.-H.M.; Abnosi, M.H. Boron Induces Early Matrix Mineralization via Calcium Deposition and Elevation of Alkaline Phosphatase Activity in Differentiated Rat Bone Marrow Mesenchymal Stem Cells. *Cell J.* **2016**, *18*, 62–73.
32. Witek, L.; Tovar, N.; Lopez, C.; Morcos, J.; Bowers, M.; Petrova, R.; Coelho, P. Assessing osseointegration of metallic implants with boronized surface treatment. *Med. Oral Patol. Oral Cir. Bucal* **2020**, *25*, e311–e317. [[CrossRef](#)] [[PubMed](#)]
33. Zhang, Y.; Chen, X.; Miron, R.; Zhao, Y.; Zhang, Q.; Wu, C.; Geng, S. In vivo experimental study on bone regeneration in critical bone defects using PIB nanogels/boron-containing mesoporous bioactive glass composite scaffold. *Int. J. Nanomed.* **2015**, *10*, 839–846. [[CrossRef](#)]

34. Routray, I.; Ali, S. Boron Induces Lymphocyte Proliferation and Modulates the Priming Effects of Lipopolysaccharide on Macrophages. *PLoS ONE* **2016**, *11*, e0150607. [[CrossRef](#)]
35. Sabaliauskas, V.; Juciute, R.; Bukelskiene, V.; Rutkunas, V.; Trumpaite-Vanagiene, R.; Puriene, A. In vitro evaluation of cytotoxicity of permanent prosthetic materials. *Stomatologija* **2011**, *13*, 75–80. [[PubMed](#)]
36. Messer, R.L.; Lucas, L.C. Cytotoxicity of nickel-chromium alloys: Bulk alloys compared to multiple ion salt solutions. *Dent. Mater.* **2000**, *16*, 207–212. [[CrossRef](#)]
37. Wataha, J.C.; Ratanasathien, S.; Hanks, C.T.; Sun, Z. In vitro IL-1 $\beta$  and TNF- $\alpha$  release from THP-1 monocytes in response to metal ions. *Dent. Mater.* **1996**, *12*, 322–327. [[CrossRef](#)]
38. Stio, M.; Martinesi, M.; Treves, C.; Borgioli, F. In vitro response of human peripheral blood mononuclear cells to AISI 316L austenitic stainless steel subjected to nitriding and collagen coating treatments. *J. Mater. Sci. Mater. Electron.* **2015**, *26*, 100. [[CrossRef](#)] [[PubMed](#)]